

LARGE HCO^+ AND HCN ABUNDANCES IN THE TRANSLUCENT CLOUD TOWARD PKS 0528+134

MICHEL R. HOGERHEIJDE

Sterrewacht Leiden, P.O. Box 9513, 2300 RA Leiden, The Netherlands

EUGÈNE J. DE GEUS

Owens Valley Radio Observatory, California Institute of Technology 105-24, Pasadena, CA 91125

MARCO SPAANS

Sterrewacht Leiden, P.O. Box 9513, 2300 RA Leiden, The Netherlands

HUIB JAN VAN LANGEVELDE¹

Joint Institute for VLBI in Europe, Radiosterrenwacht Dwingeloo, P.O. Box 2, 7990 AA Dwingeloo, The Netherlands

AND

EWINE F. VAN DISHOECK

Sterrewacht Leiden, P.O. Box 9513, 2300 RA Leiden, The Netherlands

Received 1994 September 13; accepted 1994 December 16

ABSTRACT

Observations of ^{12}CO $J = 1-0$, ^{13}CO $1-0$, HCO^+ $1-0$, HCN $1-0$, and CS $2-1$ absorption against the quasar PKS 0528+134 obtained with the Owens Valley Millimeter Array are presented. The line of sight to this standard phase calibrator crosses the diffuse outer edge of the dark cloud B30, located in the λ Ori ring of clouds. An excitation analysis of the absorption lines and ^{12}CO $1-0$ emission yields an estimated H_2 number density of $n_{\text{H}_2} = 100\text{--}500\text{ cm}^{-3}$, which is much lower than found for lines of sight studied previously by millimeter absorption lines. Surprisingly, HCO^+ and HCN are found to have abundances relative to ^{12}CO in this diffuse cloud which are comparable to or larger than those found in dark clouds. Significant differences in line width are found between ^{12}CO , HCN, and HCO^+ which cannot be attributed to line saturation. A possible explanation for the observed abundances and line widths involving cloud turbulence and the chemistry of CH^+ is proposed. It is concluded that HCO^+ absorption lines sample low-density regions which cannot be observed in molecular emission nor in CO millimeter absorption.

Subject headings: ISM: abundances — ISM: kinematics and dynamics — ISM: molecules — line: profiles — molecular processes — turbulence

1. INTRODUCTION

Until recently, the amount of information on the chemistry of diffuse and translucent clouds was limited by the low spectral resolution of optical absorption-line studies and the usually weak millimeter emission lines of molecules other than CO. In particular, no triatomic molecule has yet been detected by optical techniques. The development of millimeter wave interferometers such as that at the Owens Valley Radio Observatory (OVRO) has opened up the possibility for absorption line studies against bright extragalactic millimeter sources, providing high spectral resolution in a wavelength region where many species have strong transitions (Marscher, Bania, & Wang 1991; Bania, Marscher, & Barvainis 1991; Lucas & Liszt 1994; Lequeux, Allen, & Guillebeau 1994; Wilson & Mauersberger 1994; de Geus & Phillips 1995).

Liszt & Wilson (1993) have searched a large number of extragalactic millimeter continuum sources for the presence of Galactic CO $J = 1-0$ emission using single dish telescopes. Lucas & Liszt (1994) present molecular absorption line observations toward three of these sources. Strong, multiple lines of ^{12}CO , ^{13}CO , HCO^+ , and HCN are detected. They conclude that the abundances of HCN and HCO^+ with respect to ^{12}CO differ by more than an order of magnitude between different lines of sight, and are surprisingly large in some cases. At radio

wavelengths, absorption lines of OH (Crutcher 1980), H_2CO (Colgan, Salpeter, & Terzian 1986), and C_3H_2 (Cox, Güsten, & Henkel 1988) have been detected in the Taurus dark cloud toward 3C123 and 3C111 indicating large abundances of these molecules as well. Recently, Liszt & Lucas (1994) reported the detection of weak HCO^+ $1-0$ emission from the diffuse cloud toward ζ Oph.

In this *Letter*, we present observations of absorption lines of ^{12}CO $1-0$ and $2-1$, HCO^+ $1-0$, and HCN $1-0$, and upper limits on ^{13}CO $1-0$ and CS $2-1$, against the quasar PKS 0528+134 obtained from the OVRO database (Scoville et al. 1993). This line of sight crosses the diffuse outer edge of the dark cloud B30 which will be shown to be less dense and probably warmer than lines of sight studied so far. It provides a unique opportunity to probe the chemistry and physics of such a different environment. In particular, a new explanation for the large HCO^+ and HCN abundances and line widths is proposed which involves CH^+ , a species which is known to be abundant in diffuse clouds from optical absorption-line observations (Gredel, van Dishoeck, & Black 1993; Crawford et al. 1994), but whose role in the chemistry of other species has not yet been recognized.

2. OBSERVATIONS

The quasar PKS 0528+134 ($\alpha_{1950.0} = 05^{\text{h}}28^{\text{m}}06^{\text{s}}.8$, $\delta_{1950.0} = +13^{\circ}29'42''$) is a standard phase calibrator at

¹ Temporarily at NRAO AOC.

OVRO. The line of sight to it crosses the outer edge of the dark cloud B30, part of the λ Ori ring of clouds (Maddalena & Morris 1987), 1.5 (~ 10 pc) north of the bright rim compressed by the S264 H II region.

The observations of 0528+134 used in this Letter were obtained between 1993 September and 1994 May with a typical spatial resolution of 5". Phase calibration was obtained by self-calibration, and fluxes of 5 Jy at 3 mm and 2.5 Jy at 1.3 mm were assumed. The derived optical depths and the subsequent analysis are independent of the assumed flux. The shape of the passband was flattened by dividing by a polynomial fit of third order or less to the average spectrum of 3C273 or 3C454.3. This procedure resulted in very flat baselines; the Galactic emission and absorption found toward 3C454.3 (Liszt & Wilson 1993, de Geus & Phillips 1995) does not fall in the V_{LSR} range of the spectra. The spectral resolution ranges from 0.10 to 0.35 km s⁻¹. It is assumed that the extended emission is completely resolved out by the interferometer.

Detection of ¹²CO 1-0 emission has been reported by Liszt & Wilson (1993) using the NRAO 12 m telescope (beam size 60"). Moore et al. (1995) observed H₂CO 1₁₀-1₁₁ absorption at centimeter wavelengths.

3. RESULTS

The observed spectra are presented in Figure 1. Parameters of Gaussian profile fits to the observed spectra are given in Table 1. The absorption lines of ¹²CO, HCO⁺, and HCN occur at $V_{\text{LSR}} = 9.5 \pm 0.1$ km s⁻¹. Only two of the three hyperfine components of HCN fall completely in the passband, the third lies at the edge. No absorption has been detected of ¹³CO 1-0 and CS 2-1. The ¹²CO 1-0 absorption line with a FWHM of 0.76 km s⁻¹ is only marginally resolved at the resolution of 0.35 km s⁻¹, but is consistent with the fully resolved emission profile of 0.80 km s⁻¹ FWHM (Liszt & Wilson 1993). The HCO⁺ 1-0 spectrum shows a second, shallow absorption feature at $V_{\text{LSR}} = 2.1$ km s⁻¹. No counterpart is present in ¹²CO 1-0 absorption or emission at this position, but emission at this V_{LSR} is found 2' south (Liszt & Wilson 1993).

Although similar optical depths are derived for ¹²CO and HCO⁺, significantly different line widths of 0.76 and 1.30 km s⁻¹ FWHM are found at the respective resolutions of 0.35 and

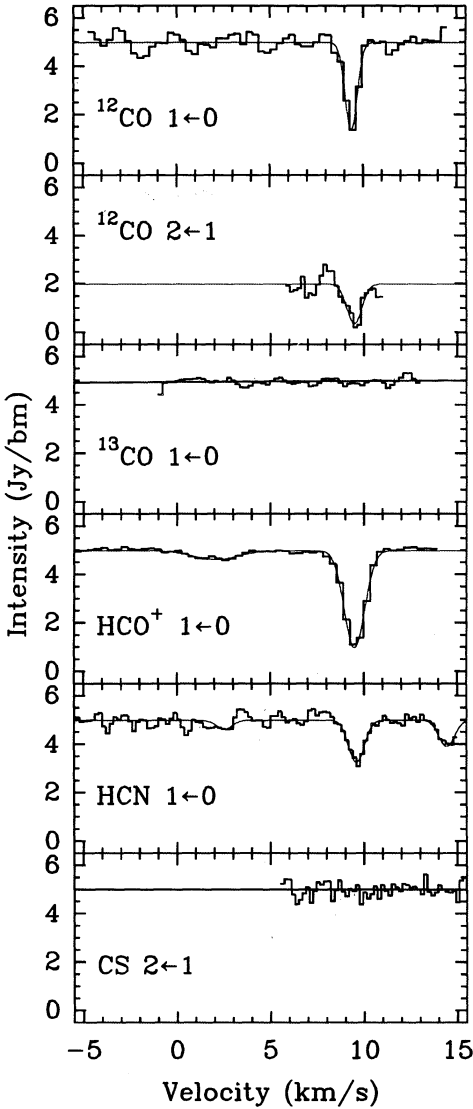


FIG. 1.—Spectra obtained toward PKS 0528+134 with the Owens Valley Millimeter Array. Horizontal scale is V_{LSR} in km s⁻¹, vertical scale is intensity in janskys per beam.

TABLE 1
ABSORPTION-LINE PARAMETERS AND INFERRED COLUMN DENSITIES

Species	V_{LSR} (km s ⁻¹)	ΔV (km s ⁻¹)	τ	N^a (cm ⁻²)	N/N_{CO}
¹² CO 1-0	9.40	0.76	1.33 ± 0.20	$(1.5-6.0) \times 10^{15}$	$\equiv 1$
	2.10	...	<0.06	$<5.0 \times 10^{13}$	$\equiv 1$
¹² CO 2-1	9.60	0.92	$1.37^{+1.56}_{-0.58}$
¹³ CO 1-0	<0.05	$<4.0 \times 10^{14}$	<0.26
HCO ⁺ 1-0	9.53	1.30	1.49 ± 0.08	$(2.3 \pm 0.1) \times 10^{12}$	$(3.6-16.0) \times 10^{-4}$
	2.10	2.8	0.08 ± 0.01	$(2.6 \pm 0.1) \times 10^{11}$	$>5.0 \times 10^{-3}$
HCN 1,2-0,1	9.61	1.06	0.44 ± 0.07	$(1.8 \pm 0.3) \times 10^{12}$	$(3.5-14.0) \times 10^{-4}$
HCN 1,1-0,1	1.26	0.24 ± 0.07
HCN 1,0-0,1	0.84	0.10 ± 0.05
CS 2-1	<0.13	$<1.0 \times 10^{12}$	$<6.7 \times 10^{-4}$
H ₂ CO 1 ₁₀ -1 ₁₁	9.5	...	0.021 ± 0.007	$>6.0 \times 10^{12}^b$	$>1 \times 10^{-4}$

^a Column densities derived using $n_{\text{H}_2} = 100-500$ cm⁻³, $T_{\text{kin}} = 20-60$ K, $x_e = 5 \times 10^{-5}$.

^b Lower limit neglecting electron collisions.

0.42 km s⁻¹. Contaminating CO emission in the interferometer beam would only aggravate the discrepancy. The main line of HCN has a width of 1.1 km s⁻¹ (resolution 0.21 km s⁻¹) but an optical depth of only 0.44. Therefore the observed differences in line width cannot be attributed to line saturation. In § 4 an explanation in terms of turbulence and cloud chemistry is proposed.

An escape probability code has been used to derive the H₂ number density n_{H_2} , the kinetic temperature T_{kin} , and the molecular column densities, including collisions with H₂ and electrons. Details of the code and references to the adopted cross sections can be found in Jansen, van Dishoeck, & Black (1994). It is assumed in these calculations that all hydrogen is in molecular form. An electron fraction $x_e = n_e/n_{\text{H}_2} = 5 \times 10^{-5}$ has been assumed, which is expected to be a reasonable average of the variation of x_e with depth into a translucent cloud (Gredel, van Dishoeck, & Black 1994). From the observed ¹²CO emission and absorption, the density is constrained to $n_{\text{H}_2} = 100\text{--}500 \text{ cm}^{-3}$, and the ¹²CO column density to $N = (1.5\text{--}5.0) \times 10^{15} \text{ cm}^{-2}$, assuming that the physical characteristics in the 5" and 60" beams are equal (see Fig. 2). The ¹²CO 1–0 antenna temperature from Liszt & Wilson (1993) has been corrected for main beam efficiency only. Because of its small dipole moment, electron collisions are unimportant for CO. Since the $J = 1$ and $J = 2$ levels are located at 5.5 K and 16.6 K above the ground level respectively, the kinetic temperature has no great influence on the excitation. The observed ¹²CO 2–1 optical depth constrains the kinetic temperature to $\gtrsim 20$ K. The inferred density of a few hundred cm⁻³ is typical for translucent clouds (van Dishoeck & Black 1989) and is an order of magnitude lower than that inferred for the lines of sight studied by Lucas & Liszt (1994).

HCO⁺, HCN and CS have much larger dipole moments than CO, but the inferred n_{H_2} is two or three orders of magni-

tude smaller than the critical density of the observed transitions. Their excitation is therefore dominated by the 2.73 K background radiation field, and hence the derived column densities are largely insensitive to variations in x_e . Only for H₂CO does the uncertainty in x_e prohibit an accurate determination of the column density. In Table 1 the inferred column densities and upper limits are listed. The predicted corresponding antenna temperatures for HCO⁺ and HCN emission are ~ 0.03 and ~ 0.01 K, respectively.

4. DISCUSSION

In dark clouds like TMC-1 abundances of HCO⁺/¹²CO and HCN/¹²CO of $(1\text{--}3) \times 10^{-4}$ are found. It is therefore remarkable that in this translucent, low density cloud values as high as $(2.5\text{--}14.0) \times 10^{-4}$ and $(3.6\text{--}16.0) \times 10^{-4}$, respectively, are inferred. For other lines of sight Lucas & Liszt (1994) reach similar conclusions. For the velocity component at $V_{\text{LSR}} = 2.1 \text{ km s}^{-1}$ an even larger value of $\text{HCO}^+/\text{CO} > 5 \times 10^{-3}$ is found assuming similar conditions as for the 9.5 km s⁻¹ component. Although such large abundance ratios could be partially due to a low CO abundance because a large fraction of carbon is atomic, the absolute column densities of HCO⁺ and HCN are much higher than can be explained by current chemical models.

Chemical models are constrained by the number density of hydrogen nuclei $n = n_{\text{H}} + 2n_{\text{H}_2}$, the gas kinetic temperature T_{kin} , the H₂ column density N_{H_2} , the intensity of the incident ultraviolet radiation field I_{UV} , and the elemental depletions. Assuming that most hydrogen is molecular, n is found from the ¹²CO excitation. An H₂ column density of $(1.0 \pm 0.5) \times 10^{21} \text{ cm}^{-2}$ is adopted based on the observed integrated CO emission with the conversion factor of Bloemen (1989), and on the 100 μm IRAS flux (de Vries & le Poole 1985) combined with the A_{ν}/N conversion of Savage et al. (1977). The incident radiation field is assumed to be enhanced by a factor of 2 with respect to the average interstellar radiation field, $I_{\text{UV}} = 2$, which is not implausible given the vicinity of the λ Ori association. The elemental depletions found toward ζ Oph are adopted (Cardelli et al. 1993; Savage, Cardelli, & Sofia 1992).

It is proposed that cloud turbulence can explain both the observed high abundances and the line widths of HCO⁺ and HCN (Spaans, Black, & van Dishoeck 1995). In the first part of Table 2 the results of chemical modeling without turbulence are presented for a number of molecules, using $n = 250 \text{ cm}^{-3}$, $T_{\text{kin}} = 60 \text{ K}$, $N_{\text{H}_2} = 1.0 \times 10^{21} \text{ cm}^{-2}$, and $I_{\text{UV}} = 2$. For these

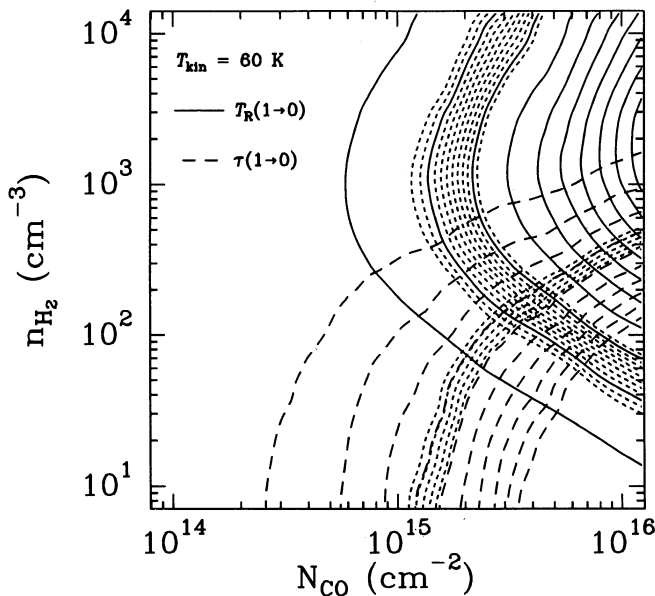


FIG. 2.—Contour plots of ¹²CO 1–0 emission (solid line) and line center optical depth (long-dashed line) as functions of ¹²CO column density and H₂ number density for $T_{\text{kin}} = 60 \text{ K}$. Contour levels are $T_{\text{R}} = 1.0, 2.0, \dots, \text{K}$, and $\tau = 0.3, 0.6, \dots, 3.0$. Observed values are indicated with their respective errors by the short-dashed lines. For the lowest temperature consistent with the observations, $T_{\text{kin}} = 20 \text{ K}$, the inferred n_{H_2} is enhanced by about a factor of 2.

TABLE 2
RESULTS OF “QUIESCENT” AND TURBULENT
CHEMICAL MODELS

SPECIES	N (cm ⁻²)	
	$\Delta V_{\text{turb}} = 0$	$\Delta V_{\text{turb}} = 3.5 \text{ km s}^{-1}$
¹² CO	5.5×10^{14}	2.3×10^{15}
¹³ CO	4.7×10^{13}	6.6×10^{13}
CH ⁺	2.2×10^{11}	5.1×10^{13}
CH	3.2×10^{13}	9.5×10^{13}
C ₂ H	3.5×10^{13}	9.6×10^{13}
HCO ⁺	8.2×10^9	8.1×10^{11}
HCN	7.2×10^9	9.3×10^{11}
CS	1.2×10^{10}	1.9×10^{11}
CN	1.1×10^{13}	3.9×10^{13}
H ₂ CO	1.4×10^8	2.4×10^8

parameters the model clearly fails to produce the observed amounts of HCO^+ and HCN by two orders of magnitude. Even for the highest density consistent with the observations, $n = 10^3 \text{ cm}^{-3}$, the produced column densities of HCO^+ and HCN are not significantly increased.

The second part of Table 2 gives the results for chemical modeling including the effects of turbulence for the same cloud parameters. A turbulent velocity structure differs from a pure Gaussian shape by excess power in the line wings, as has been observed toward dark clouds (Falgarone & Phillips 1990). Spaans et al. (1995) discuss the possible formation of the observed large amounts of CH^+ in diffuse clouds in general through the endoergic reaction $\text{C}^+ + \text{H}_2 \rightarrow \text{CH}^+ + \text{H}$, where turbulence provides the translational energy needed to overcome the reaction barrier. A relatively high fraction of CH^+ is produced with a large velocity dispersion. Since CH^+ is rapidly converted to CH_2^+ it cannot thermalize by elastic collisions with H_2 , explaining its observed broad line profiles (Lambert, Sheffer, & Crane 1990). It is proposed here that any species whose formation involves CH^+ will inherit part of this broad velocity distribution provided that both the formation and the destruction proceed on timescales shorter than that needed for thermalization. The formation of both HCO^+ and HCN involves CH^+ through the reactions $\text{CH}^+ + \text{O} \rightarrow \text{CO}^+ + \text{H}$; $\text{CO}^+ + \text{H}_2 \rightarrow \text{HCO}^+ + \text{H}$ and $\text{CH}_2^+ + \text{N} \rightarrow \text{HCN}^+ + \text{H}$; $\text{HCN}^+ + \text{H}_2 \rightarrow \text{H}_2\text{CN}^+ + \text{H}$; $\text{H}_2\text{CN}^+ + e \rightarrow \text{HCN} + \text{H}$. Another, less important HCO^+ formation channel is through the $\text{C}^+ + \text{OH}$ reaction, where OH is enhanced because the rates for the endoergic reactions $\text{O} + \text{H}^+ \rightarrow \text{O}^+ + \text{H}$ and $\text{O} + \text{H}_2 \rightarrow \text{OH} + \text{H}$ are increased by turbulence as well. Spaans et al. (1995) present the results of a parameter study of the effects of turbulence on the chemistry. The critical input parameter is ΔV_{turb} , a measure of the total kinetic energy per unit mass injected into the medium on the largest scales. Resulting line profile widths are calculated by making simple assumptions about the redistribution of translational energy in subsequent reactions, and by assuming a FWHM of 0.80 km s^{-1} for the "quiescent" gas. For $\Delta V_{\text{turb}} = 3.5 \text{ km s}^{-1}$, the resulting line widths are $\Delta V(\text{HCO}^+) = 1.5 \text{ km s}^{-1}$, $\Delta V(\text{HCN}) = 1.1 \text{ km s}^{-1}$ and $\Delta V(^{12}\text{CO}) = 0.9 \text{ km s}^{-1}$, convolved with the respective instrumental resolutions (§ 3). It can be seen that this model explains the observed line widths and column densities reasonably well for the derived param-

eters. In particular, HCO^+ and HCN are enhanced by one to two orders of magnitude, and even CO is increased by a factor of 4. Note that the enhanced CO abundance also leads to additional HCO^+ through the $\text{CO} + \text{H}_3^+$ reaction. Although the detailed results depend sensitively on the adopted parameters, the computed trends are robust. Only for H_2CO are the predicted column densities too low by several orders of magnitude, but grain surface reactions, which could be important, have not been included. The adopted value of ΔV_{turb} is a factor of 2 larger than the values inferred by Gredel et al. (1994) for high-latitude clouds, which is not unexpected since the compression of B30 on one side by the expanding hot gas of S264 deposits large amounts of energy in the cloud.

We conclude that in this low-density, diffuse cloud, the turbulence influences the cloud chemistry dramatically, as reflected in the high HCO^+ and HCN abundances and their line profiles. For densities $n > 10^3 \text{ cm}^{-3}$ the CH^+ formation is strongly suppressed, since the mean free path on which C^+ reacts with H_2 to form CH^+ becomes less than the scale length on which the turbulence is dissipated. It is therefore only in low-density clouds such as this one that the effects of turbulence on the chemistry become apparent. Liszt & Lucas (1994) report similar column densities of ^{12}CO and HCO^+ toward ζ Oph, a line of sight of similar physical conditions. The measured CH^+ column density toward ζ Oph is of the same order of magnitude as predicted for our line of sight. The observations presented by Lucas & Liszt (1994) show velocity components with very broad HCO^+ and HCN profiles in the absence of ^{12}CO emission, suggesting very low densities. This shows that searches for molecular absorption should not be limited to lines of sight with detected CO emission. Because of its high dipole moment and relatively large abundance, HCO^+ samples low-density regions which cannot be observed in molecular emission nor in CO millimeter absorption.

This work was supported by a PIONIER grant of the Netherlands Organization for Scientific Research (NWO). The Owens Valley Millimeter Array is operated under funding from NSF grant AST 93-14079, which also supports EdG. The authors thank A. Marscher for communicating the H_2CO results before publication and providing valuable comments on the manuscript, and J. H. Black and H. S. Liszt for useful discussions.

REFERENCES

- Bania, T. M., Marscher, A. P., & Barvainis, R. 1991, *AJ*, 101, 2147
 Bloemen, J. B. G. M. 1989, *ARA&A*, 27, 469
 Cardelli, J. A., Mathis, J. S., Ebbets, D. C., & Savage, B. D. 1993, *ApJ*, 402, L17
 Colgan, S. W. J., Salpeter, E. E., & Terzian, Y. 1986, *AJ*, 91, 107
 Cox, P., Güsten, R., & Henkel, C. 1988, *A&A*, 206, 108
 Crawford, I. A., Barlow, M. J., Diego, F., & Spyromilio, J. 1994, *MNRAS*, 266, 903
 Crutcher, R. M. 1980, *ApJ*, 239, 549
 de Geus, E. J., & Phillips, J. A. 1995, *ApJL*, submitted
 de Vries, C. P., & le Poole, R. S. 1985, *A&A*, 145, L7
 Falgarone, E., & Phillips, T. G. 1990, *ApJ*, 459, 344
 Gredel, R., van Dishoeck, E. F., & Black, J. H. 1993, *A&A*, 269, 477
 ———. 1994, *A&A*, 285, 300
 Jansen, D. J., van Dishoeck, E. F., & Black, J. H. 1994, *A&A*, 282, 605
 Lambert, D. L., Sheffer, Y., & Crane, P. 1990, *ApJ*, 359, L19
 Lequeux, J., Allen, R. J., & Guilloteau, S. 1994, *A&A*, 280, L23
 Liszt, H. S., & Lucas, R. 1994, *ApJ*, 431, L131
 Liszt, H. S., & Wilson, R. W. 1993, *ApJ*, 403, 663
 Lucas, R., & Liszt, H. S. 1994, *A&A*, 282, L5
 Maddalena, R. J., & Morris, M. 1987, *ApJ*, 323, 179
 Marscher, A. P., Bania, T. M., & Wang, Z. 1991, *ApJ*, 371, L77
 Moore, E. M., et al. 1995, in preparation
 Savage, B. D., Bohlin, R. C., Drake, J. F., & Budich, W. 1977, *ApJ*, 216, 291
 Savage, B. D., Cardelli, J. A., & Sofia, U. J. 1992, *ApJ*, 401, 706
 Scoville, N. Z., Carlstrom, J. E., Chandler, C. J., Phillips, J. A., Scott, S. L., Tilanus, R. P. J., & Wang, Z. 1993, *PASP*, 105, 1482
 Spaans, M., Black, J. H., & van Dishoeck, E. F. 1995, *ApJ*, submitted
 van Dishoeck, E. F., & Black, J. H. 1989, *ApJ*, 340, 273
 Wilson, T. L., & Mauersberger, R. 1994, *A&A*, 282, L41